Available online at www.sciencedirect.com
SCIENCE DIRECT®
Journal of Colloid and Interface Science 276 (2004) 13–23
JOURNAL OF Colloid and Interface Science
www.elsevier.com/locate/jcis

Effect of iron oxide coatings on zinc sorption mechanisms at the clay-mineral/water interface

Maarten Nachtegaal [*,1] and Donald L. Sparks

Molecular Environmental Soil Chemistry Group, Department of Plant and Soil Sciences, University of Delaware, 152 Townsend Hall, Newark, DE 19717-1303, USA

Received 10 October 2003; accepted 11 March 2004

Available online 16 April 2004

Abstract

Oxide surface coatings are ubiquitous in the environment, but their effect on the intrinsic metal uptake mechanism by the underlying mineral surface is poorly understood. In this study, the zinc (Zn) sorption complexes formed at the kaolinite, goethite, and goethite-coated kaolinite surfaces, were systematically studied as a function of pH, aging time, surface loading, and the extent of goethite coating, using extended X-ray absorption fine structure (EXAFS) spectroscopy. At pH 5.0, Zn partitioned to all sorbents by specific chemical binding to hydroxyl surface sites. At pH 7.0, the dominant sorption mechanism changed with reaction time. At the kaolinite surface, Zn was incorporated into a mixed metal Zn–Al layered double hydroxide (LDH). At the goethite surface, Zn initially formed a monodentate inner-sphere adsorption complex, with typical Zn–Fe distances of 3.18 Å. However, with increasing reaction time, the major Zn sorption mechanism shifted to the formation of a zinc hydroxide surface precipitate, with characteristic Zn–Zn bond distances of 3.07 Å. At the goethite-coated kaolinite surface, Zn initially bonded to FeOH groups of the goethite coating. With increasing aging time however, the inclusion of Zn into a mixed Zn–Al LDH took over as the dominant sorption mechanism. These results suggest that the formation of a precipitate phase at the kaolinite surface is thermodynamically favored over adsorption to the goethite coating. These findings show that the formation of Zn precipitates, similar in structure to brucite, at the pristine kaolinite, goethite, and goethite-coated kaolinite surfaces at near neutral pH and over extended reaction times is an important attenuation mechanism of metal contaminants in the environment.

Keywords: Coating; Zinc; Sorption; XAFS; Goethite; Kaolinite; Surface precipitation

1. Introduction

The bioavailability and migration of trace metals in the environment is dictated by reactions taking place at soil solution–particle interfaces [1–3]. Determining the kinetics and mechanisms of these interfacial reactions is of utmost importance to insure the implementation of sound remediation strategies, to predict metal stability in soils over time, and to successfully model the fate of trace metals in soils.

The type and stability of metal sorption complexes formed at solution–particle interfaces depend on the solution conditions (pH and ionic strength) and the solid phase present. Phyllosilicates and metal-(oxy)hydroxides are among the most reactive minerals in the environment [4]. The sorption mechanisms of metals on these individual sorbents are reasonably well understood. However, many metal oxides and oxyhydroxides, including iron oxides (i.e., ferrihydrite, goethite, and hematite) occur in the environment as reactive surface coatings on phyllosilicates. These coatings, often discrete particles in the nanosize range, are the result of weathering of primary minerals and subsequent reprecipitation [5]. Little is known on the effect of metal oxide coatings on the intrinsic sorption mechanisms of trace metals to clay mineral surfaces, although in the most extreme scenarios these coatings could dictate metal uptake instead of the underlying clay mineral. The presence of organic coatings [6,7] and biofilms [8] have in some instances been shown to affect total metal uptake by the mineral surfaces, but not to change the intrinsic metal uptake mechanism of the underlying mineral surface.

* Corresponding author. Fax: +41-1-633-1123.
E-mail address: nachtegaal@env.ethz.ch (M. Nachtegaal).
[1] Present address: Maarten Nachtegaal Institute for Terrestrial Ecology (ITÖ), Swiss Federal Institute of Technology (ETH), Grabenstrasse 3, CH-8952 Schlieren, Switzerland.

0021-9797/$ – see front matter
doi:10.1016/j.jcis.2004.03.031

Among potentially toxic trace metals, zinc (Zn) is one of the most widespread contaminants in the environment [9]. It accumulates in soils by atmospheric deposition originating from smelting operations and by agricultural applications of sewage sludge and agrochemicals [10–13]. Zinc plays an essential role in cellular systems and enzymes [14]. A deficiency of Zn in animals and humans can lead to anorexia and growth depression [14]. Although Zn is relatively non-toxic, elevated levels of Zn are detrimental to the environment. At acidic pH values, Zn toxicity to plants is the third most common after Al and Mn [15].

The partitioning of Zn to phyllosilicate minerals has been extensively studied, see for example reviews in [1,4]. In acidic to near neutral environments, Zn partitioning to phyllosilicate surfaces mainly occurs by electrostatic interactions, due to a net negative structural charge developed within the octahedral layers of phyllosilicates (due to isomorphic substitutions), and by specific chemical binding to hydroxyl edge sites. At higher solute concentrations and pH > 6.5, Zn, similar to Ni and Co, can be incorporated into neo-formed precipitates, formed at the surfaces of phyllosilicate minerals [16–19]. These surface precipitates form at solution conditions undersaturated with respect to homogeneous precipitation. Depending on the type of phyllosilicate mineral present, initially a mixed metal–Al layered double hydroxide (Me–Al LDH) is formed, with the structural formula generally written as $[Me^{2-}_{1-x}Me^{3+}_{x}(OH)_2]^{x+}\cdot(x/n)A^{n-}\cdot mH_2O]$. Interestingly, with increasing reaction time, the anionic species in the interlayer space of the LDH can be replaced by silica polymers transforming the LDH gradually into a more stable precursor Me–Al phyllosilicate [19]. And therefore, the incorporated metal becomes increasingly stable with respect to weathering [19,20]. Thus, the incorporation of metals into neo-formed surface precipitates could potentially lead to a long term sequestration of the bioavailable metal fraction in the environment at neutral pH [12].

Goethite (α-FeOOH) is one of the most common iron oxides in soils [21] and often occurs as coatings on clay minerals [22]. Macroscopic and spectroscopic studies have shown that Zn partitioning to goethite at neutral pH mainly occurs by chemisorption [23–25]. Coughlin and Stone [26] however, found an increasingly stable fraction of Co, Ni, and Cu sorbed to goethite with aging. It was proposed that, similar to the formation of Me–Al LDH precipitates on clay mineral surfaces, micro-scale formation of metal spinels, $(Me^{2+}, Fe^{2+})Fe^{3+}_2O_4$, at the goethite surface may have caused the net increase in sorption and the subsequent decrease in the ability to desorb partitioned metals. Although in our systems no Fe^{2+} is added, and thus the formation of spinel is warranted, the possibility of the formation of Zn containing surface precipitates with longer reaction time was investigated further.

In this paper we systematically investigated the effect of crystalline iron oxide (goethite) coatings on the mechanisms of Zn sorption to kaolinite, an ideal 1:1 clay mineral, in order to obtain a better understanding of the effect of metal oxide coatings on the intrinsic metal sorption mechanism to clay minerals. A heterogeneous suspension reaction was used to obtain a stable goethite coating at the kaolinite surface [27]. The advantage of using this method is that the resulting surface coating consists of crystallographically pure and well-characterized goethite in contrast to traditional coating methods, where iron oxide coated clay particles are synthesized by adding base to an acidic Fe(III) solution in the presence of the clay [28,29]. The sorption complexes formed at the goethite-coated kaolinite surface and the individual sorbents are delineated using XAFS spectroscopy and systematically studied as a function of pH (5 and 7), aging time, and surface loading.

2. Materials and methods

2.1. Materials

The kaolinite used in this study was a well-crystallized Georgia kaolinite (Clay Mineral Society source clay, KGa-1). Carbonates and exchangeable divalent ions were removed from the kaolinite by reaction with a NaOAc buffer at pH 5 in a near boiling water bath [30]. Organic matter was removed by treating the kaolinite with H_2O_2. Iron oxides were removed with a dithionite–citrate–bicarbonate mixture in a 80 °C warm water bath. The resulting kaolinite was washed twice with 1 M NaCl, and twice with DI water to convert the clay into the homoionic Na form. The <0.2 μm fraction was separated by centrifugation, dialyzed against DI water, and freeze-dried. The specific surface area of the resulting kaolinite was determined by a five point N_2 Brunauer–Emmett–Teller (BET) gas adsorption isotherm method and was 14.01 $m^2\,g^{-1}$.

A well defined goethite was synthesized according to the method outlined in Schwertmann et al. [21] and modified by Peak et al. [31]. Initially, ferrihydrite was precipitated by adding 50 ml of a 1 M ferric nitrate solution to 450 ml of 1 M KOH. The suspension of amorphous hydrous ferric oxide was aged for 21 days at 25 °C to obtain crystalline goethite. This suspension was washed via centrifugation, where the supernatant was replaced with DI water to remove residual KOH. The rinsed solid was re-suspended in 0.4 M HCl and shaken for 2 h using a mechanical shaker [31]. This treatment was used to remove any remaining ferrihydrite from the surface of the goethite. The acidified goethite suspension was then washed with DI water to remove HCl, dialyzed against DI water, and freeze dried. The BET surface area of the goethite was 66.49 $m^2\,g^{-1}$.

Coatings of this well-defined goethite on the kaolinite surface were prepared using the method of Scheidegger et al. [27]. Two separate batches were prepared which yielded different amounts of goethite coatings on the kaolinite surface. Essentially, 200 and 400 mg of goethite were mixed with 2.5 g of kaolinite in 200 ml of a pH 7.5 and

$I = 0.01$ M $NaNO_3$ solution. This suspension was shaken for 48 h and re-suspended three times in a $NaNO_3$ solution at the pH and ionic strength of the reaction medium (pH 7, $I = 0.1$ M $NaNO_3$). The coated kaolinite particles were washed several times with the background solution and finally with DI water. The resulting solids were oven dried at 110 °C. Four samples (100 mg each) of the coated kaolinite were dissolved in 2 ml HNO_3 (95%) and 1 ml HF (40%) to determine the extent of the goethite coating. Al and Fe concentrations in the clear solution were measured on a Finnigan ELEMENT 1 high resolution magnetic sector inductively coupled plasma mass spectrometer (HR-ICP-MS) at the National High Magnetic Field Laboratory (Tallahassee, FL). A mass balance indicated that 6.1 and 10.7 weight percent goethite was coated on the kaolinite surface by this method. The BET surface areas of the resulting goethite-coated kaolinite were 16.56 and 22.01 $m^2\,g^{-1}$, respectively. The extent of coating was also checked with scanning electron microscopy (SEM) using a Hitachi SEM S4700 at the Delaware Biotechnology Institute.

2.2. Zn adsorption isotherms

Adsorption isotherms were conducted at constant pH 7 and room temperature. In 250 ml polyethylene centrifuge bottles, 100 ml of a 0.1 $g\,L^{-1}$ kaolinite, goethite, or 10 wt% goethite-coated kaolinite suspensions were equilibrated at pH 7 for 24 h under constant agitation. Zinc was then added from an acidified 0.1 M $Zn(NO_3)_2$ solution, to achieve initial Zn concentrations ranging from 0.01–1.0 mM. The initial zinc concentrations were chosen below the solubility of Zn hydroxide, but for the 0.8–1.0 mM samples they might have been above the solubility of Zn–Al LDH and Zn carbonate [16]. A 0.05 M 2-4-(morpholino)ethanesulfonic acid (MES) buffer was used to maintain a constant pH. This buffer does not interfere with metal sorption [32]. All experiments were performed in a glove box at a nitrogen atmosphere, to prevent the formation of Zn-carbonates and hydrozincite. After centrifugation, Zn concentrations in the supernatant were analyzed with flame atomic absorption spectrometry (AAS).

2.3. Preparation of Zn sorption samples for XAFS

Zinc sorption to kaolinite, goethite, and a goethite-coated kaolinite were studied as a function of pH, surface loading, and aging time. All sorption experiments were performed in a glove box at constant pH, using a 0.05 M MES buffer, and constant ionic strength (0.1 M $NaNO_3$). At pH 5, maximum loading samples were prepared by reacting 3 mM Zn with 10 g solid L^{-1}. At pH 7, the solid suspension density, reaction time and initial [Zn] were varied to achieve a range of loading levels (Table 1). To study the effect of reaction time at pH 7, a new batch was prepared with a suspension density of 10 g solid L^{-1} and an initial [Zn] of 1 mM. Zinc from a 0.1 M $Zn(NO_3)$ stock solution was added in small increments. These resulting suspensions were placed on a reciprocal shaker for 46 days. At day 4 and 46, samples were collected for EXAFS analysis. All Zn reacted solids were separated from suspension via vacuum filtration through a 0.2 µm filter to minimize the entrapment of aqueous Zn. The resulting wet pastes were immediately loaded into acrylic sample holders, which were sealed with Kapton polyamide tape (CHR Industries, type K-104) to avoid moisture loss during analysis. The supernatants were analyzed on flame AAS for Zn, to determine surface loading levels.

2.4. Preparation of reference compounds for EXAFS analysis

A solvated $Zn^{2+}_{(aq)}$ reference was prepared by dissolving $Zn(NO_3)_2$ in DI water to obtain a total Zn concentration of 15 mM. The pH was adjusted to 5 to prevent polymerization. A synthetic mixed Zn–Al layered double hydroxide (LDH) reference was prepared at pH 6.3 using the method of Taylor [33]. The final precipitate had a Zn:Al ratio of 1.7 based on total dissolution of the solid and measurement of dissolved Zn and Al by flame AAS [16].

2.5. XAFS data collection and analysis

X-ray absorption spectra were collected at beamline X-11A of the National Synchrotron Light Source (NSLS), Brookhaven National Laboratory, Upton NY. The electron storage ring operated at 2.8 GeV with an average beam current of 180 mA. The monochromator consisted of two parallel Si (111) crystals with an entrance slit of 0.5 mm. Higher order harmonics were suppressed by detuning 30% from the maximum beam intensity. The monochromator position was calibrated by assigning the first inflection point on the K-edge of a zinc metal foil to 9659.0 eV. The spectra were collected in fluorescence mode using an Ar-filled Lytle detector. Two sheets of Al (when Fe was present in the system), a 6 µm-Cu filter and soller slits were placed between the sample and the detector to reduce elastic scattering. The incoming beam was measured with a N_2-filled ion chamber. All spectra were collected at room temperature and at least three scans were collected per sample to improve the signal to noise ratio.

XAFS data reduction was performed using WinXAS 2.1 [34] following standard procedures [6,35]. The χ function was extracted from the raw data by fitting a linear function to the pre-edge region and a spline function to the post-edge region, and normalizing the edge jump to unity. The energy axis (eV) was converted to photoelectron wave vector units ($Å^{-1}$) by assigning the origin, E_0, to the first inflexion point of the absorption edge. The resulting $\chi(k)$ functions were k^3 weighted to compensate for dampening of the XAFS amplitude with increasing k and were Fourier-transformed to obtain radial structure functions (RSFs). A Bessel window with a smoothing parameter of 4 was used to suppress artifacts

Table 1
Experimental and structural parameters for Zn sorption and reference samples

	Time (d)	Γ (μmol/m^2)	$[C]_i$	s:s (g/L)	Zn–O			Zn–Zn/Fe/Al				ΔE_0 (eV)	χ^2_{res} (%)
					CN	R (Å)	σ^2 (Å)^2	Atom	CN	R (Å)	σ^2 (Å)^2		
References													
$Zn^{2+}_{(aq)}$			15		6.0	2.07	0.009					−0.45	9.04
Zn–Al LDH					6.2	2.07	0.008	Zn	4.3	3.09	0.010	0.06	19.52
								Al	2.2	3.10	0.010		
pH 5.0													
Kaolinite		1.496	3	10.0	6.6	2.07	0.011	Al	1.4	3.09	0.010	0.46	21.30
Goethite		0.183	3	10.0	5.0	2.05	0.009	Fe	2.6	3.65	0.010	−0.15	31.33
Kaol-6Goeth		0.889	3	10.0	6.6	2.06	0.015	Al	1.8	3.11	0.010	0.68	31.96
pH 7.0 surface loading													
Kaolinite	1	2.818	1	5.3	6.3	2.05	0.013	Zn	3.6	3.13	0.010	0.64	12.62
								Al	0.9	3.19	0.010		
Kaolinite	7	2.171	1	8.0	5.2	2.03	0.010	Zn	4.9	3.10	0.011	−0.26	14.78
								Al	2.6	3.12	0.010		
Goethite	1	2.033	1	5.3	6.1	2.04	0.013	Fe	0.8	3.18	0.001	0.64	28.06
Goethite	7	1.217	1	8.0	4.9	2.01	0.010	Fe/Zn	1.5	3.06	0.013	−1.87	25.12
Kaol-6Goeth†	1	1.709	1	5.3	6.7	2.04	0.014	Zn	2.0	3.15	0.012	1.71	10.67
Kaol-6Goeth†	7	1.595	1	8.0	6.0	2.05	0.013	Zn/Fe	2.8	3.13	0.010	0.78	16.52
pH 7.0 reaction time													
Kaolinite	4	1.408	1	10.0	5.5	2.02	0.013	Zn	1.2	3.10	0.010	0.22	16.77
								Al	1.0	3.09	0.010		
Kaolinite	46	1.597	1	10.0	6.2	2.03	0.010	Zn	3.9	3.11	0.010	0.76	17.38
								Al	1.8	3.14	0.010		
Goethite	4	1.260	1	10.0	6.0	2.04	0.014	Fe	1.0	3.18	0.010	0.62	19.18
Goethite	46	1.496	1	10.0	5.8	2.06	0.011	Fe/Zn	1.2	3.07	0.010	0.57	15.89
Kaol-10Goeth†	4	2.244	1	10.0	5.2	2.01	0.013	Fe	0.6	3.19	0.011	1.05	14.16
Kaol-10Goeth†	46	2.190	1	10.0	5.7	2.02	0.012	Zn/Fe	1.5	3.11	0.010	0.35	20.46
								Al	0.9	3.11	0.010		

Note. Γ = surface loading, $[Zn]_i$ = initial Zn concentration, s:s = solid:solution ratio, CN = coordination number (±30%), R (Å) = radial distance (±0.02 Å for the first shell and ±0.05 Å for the second shell), σ^2 (Å)^2 = Debye–Waller factor, ΔE_0 (eV) = phase shift, χ^2_{res} (%) = fit error, † = 6.6 wt% goethite coating and 10.7 wt% goethite coating.

due to the finite Fourier filtering range between $\Delta k \approx 1.5$–12.4 Å^{-1} for the kaolinite samples, $\Delta k \approx 1.6$–10.9 Å^{-1} for the goethite-coated kaolinite samples, and $\Delta k \approx 1.7$–11.0 Å^{-1} for the goethite samples. The two major peaks below 3.6 Å in the Fourier transformed curves were isolated and backtransformed. A R range of ≈0.7–3.6 Å was used for the first two peaks of the kaolinite samples, a R range of ≈0.8–3.6 Å was used for the goethite-coated kaolinite samples, and a R range of ≈0.8–3.2 Å was employed for the goethite samples. These backtransformed peaks were fit in k space. Structural parameters were extracted with fits to the standard EXAFS equation. Ab initio Zn–O and Zn–Zn/Al scattering paths were generated using the FEFF 7.02 [36] code from the refinement of the structure of lizardite where Zn or Al was substituted for Mg in octahedral positions [37]. Zn–O and Zn–Zn/Fe scattering paths were generated from the refinement of Franklinite. Optimization of the parameters was performed with the energy shifts constrained to be equal and the amplitude reduction factor, $(S_0)^2$, fixed at 0.85. The value for $(S_0)^2$ was obtained from fitting Zn_{aq} and fixing the Zn–O coordination number to 6. A good fit was determined on the basis of the minimum residual error.

3. Results and discussion

3.1. Adsorption isotherms

The heterogeneous suspension reaction, used to coat crystalline goethite at the kaolinite surface, yielded goethite coatings of ∼6 and ∼10 wt%. A SEM image of this goethite-coated kaolinite, collected at a 400-fold magnification showed 0.5–1 μm large hexagonal kaolinite platelets, with 0.2–0.5 μm needle or rod shaped goethite particles coated onto the kaolinite surface (Fig. 1).

Zinc adsorption isotherms in suspensions of kaolinite, goethite, and 10 wt% goethite-coated kaolinite, are presented in Fig. 2. None of the isotherms display typical Langmuirian shape [2], with the possible exception of the goethite-coated kaolinite. Thus, site saturation could not be estimated. The steep increase for the Zn kaolinite adsorption isotherm after $C_f = 0.3$ mM Zn, suggests that a Zn containing phase was precipitating. The goethite-coated kaolinite surface seems to have a higher affinity for Zn than the kaolinite or goethite surface alone. This might be caused by the formation of extra sorption sites at the step sites created by the sorption of goethite particles onto kaolinite. No definite finding on the Zn sorption mechanisms taking place on these three solids can be derived from macroscopic data alone. EXAFS spectroscopic analysis was applied to verify the sorption mechanisms in the different regions of Fig. 2 (Table 1).

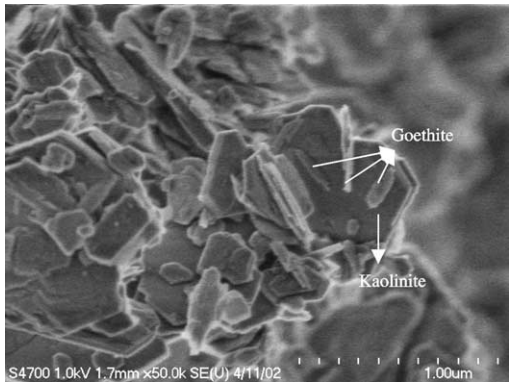

Fig. 1. SEM photograph of the goethite-coated kaolinite, taken at a 400-fold magnification. The hexagonal platelets are the kaolinite minerals and the needle shaped rods are goethite particles.

3.2. Zn sorption at pH 5

Fig. 3A shows the raw k^3-weighted χ spectra of aqueous zinc, Zn/kaolinite, Zn/goethite, and Zn/goethite-coated kaolinite sorption samples, reacted with 3 mM Zn at pH 5 for 2 days and a mixed Zn–Al layered double hydroxide (Zn–Al LDH) reference. The spectrum for Zn_{aq}^{2+} has a single wave frequency, and its amplitude monotonically decreases with increasing k. This monotonic decrease with k is consistent with the presence of a single ordered coordination sphere. In contrast, the χ spectrum of the mixed Zn–Al LDH has several distinct frequencies, resulting from multiple scattering paths of higher atomic shells. Compared to the χ spectrum of aqueous zinc, the phase of the wave frequency of the Zn sorbed samples is slightly shifted. This indicates that these spectra contain the signature of more than one atomic shell, probably due to the formation of direct bonds with the mineral surfaces. The lack of very distinct frequencies in the spectra, such as is present in the spectrum of the synthetic Zn–Al LDH, indicates that no Zn containing precipitates formed in the sorption samples. The raw χ spectra of the sorption samples, and especially of the Zn/goethite

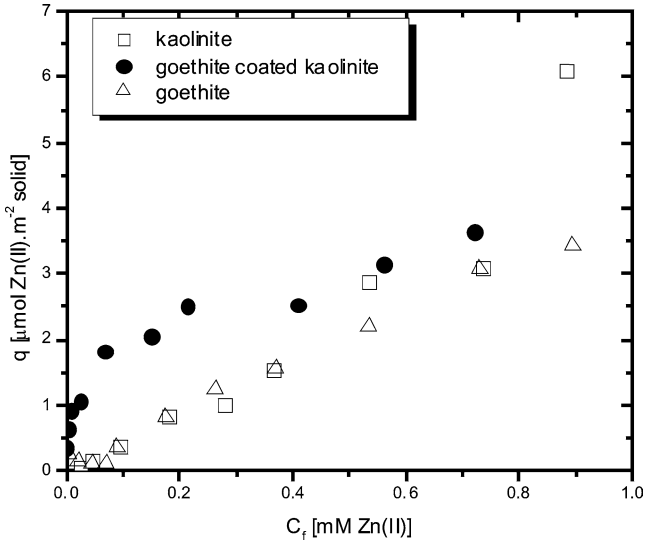

Fig. 2. Zinc adsorption isotherms conducted on kaolinite, goethite, and 10.7 wt% goethite-coated kaolinite. Experimental conditions: $T = 294$ K, pH 7.0, $I = 0.1$ M $NaNO_3$, suspension density of 0.1 g L^{-1}.

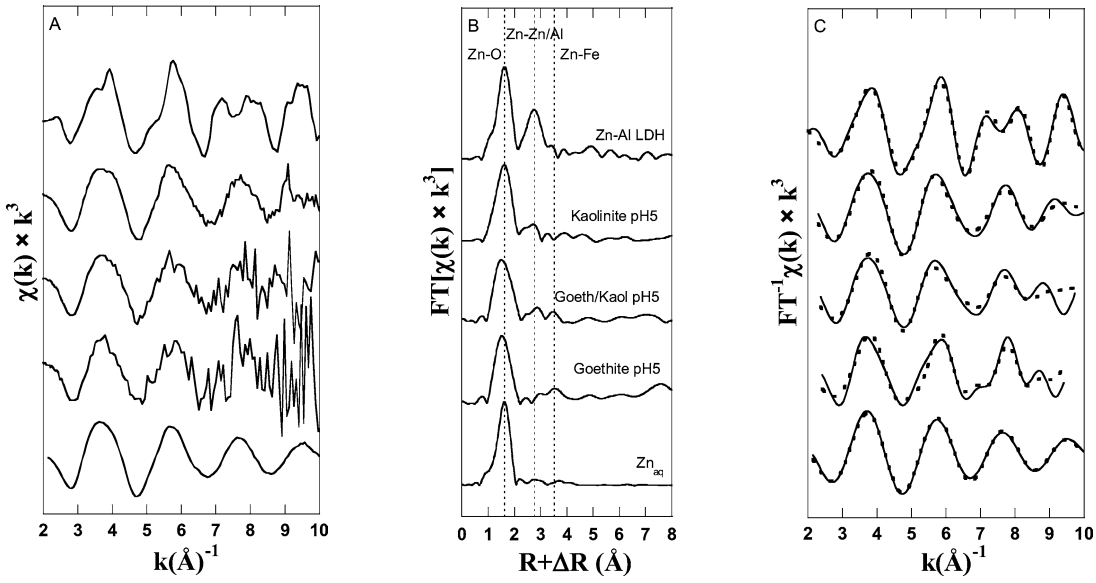

Fig. 3. (A) The k^3-weighted $\chi(k)$ of the pH 5.0 Zn adsorption samples, aqueous Zn and the synthetic Zn–Al LDH reference compound, (B) the corresponding Fourier transforms (not corrected for phase shift), and (C) the fitted inverse Fourier transform of the two first shells of the Fourier transforms, with the solid lines representing the experimental data and the dotted lines the best fits.

sorption sample, are very noisy. This is due to the fact that very little Zn could actually be sorbed onto the mineral surfaces at pH 5 (Table 1). The point of zero charge (pzc) of goethite is around 8 [4], which means that at pH 5 it is positively charged. This positive charge might repel the positively charged Zn ions away from the surface. The pzc of kaolinite lies around 5, therefore it is not repelling Zn ions and a much higher surface loading could be obtained.

Fig. 3B shows the radial structure functions (RSFs) obtained by Fourier transforming the raw χ spectra. The main peaks in the RSF were backtransformed to k space (Fig. 3C) and fit with scattering paths calculated with FEFF 7 (dashed lines). Structural parameters obtained from best fitting the backtransformed χ spectra are listed in Table 1.

The RSF of aqueous zinc, not corrected for phase shift, displays only one peak located at $R + \Delta R = 1.8$ Å, which was fitted with 6 oxygen atoms at 2.07 Å (Table 1). This coordination number and bond length is in good agreement with previous work [38] and with a sixfold coordination of Zn^{2+} by water [39]. The first peak for the Zn/goethite and Zn/goethite-coated kaolinite samples seems to be shifted to a lower radial distance, compared to Zn (aq), the Zn–Al LDH, and the Zn/kaolinite sorption sample. Zn(II) is commonly found in both four- and sixfold coordination with oxygen atoms [40]. The Zn–O first-shell coordination number is well correlated with bond length, with Zn–O bond lengths of ≈1.96 Å typical of fourfold coordination, and Zn–O bond lengths of ≈2.08 Å typical of sixfold coordination [41]. A shift of the first peak of the Zn/goethite and Zn/goethite-coated kaolinite samples to shorter bond distances, suggest that these two sorption samples have a lower coordination number than the sixfold coordination found for aqueous zinc. However, fitting results only indicated a slighter shorter (within the reported fitting error) bond length of 2.05 Å for Zn/goethite and 2.06 Å for goethite-coated kaolinite. The coordination number of approximately 6 suggests that Zn is in an octahedral environment in all sorption samples.

All three sorption samples exhibit one or two smaller peaks at larger radial distances (Fig. 3B). The second-shell feature in the Zn/kaolinite sample is best fit with ∼1 Al atom at 3.09 Å, indicating that Zn is sorbed as an inner-sphere sorption complex to aluminol groups on the edge sites of the kaolinite. In a study on the sorption mechanisms of Zn to an acidic forest soil (pH 5.5), Voegelin et al. [42] found significantly shorter Zn–Al bond distances of ∼2.99 Å and attributed these to aluminol groups on edge surfaces of either phyllosilicates or amorphous Al hydroxides. In a study on the sorption mechanisms of Zn on aluminum powders, Trainor et al. [43] found Zn–Al bond distances ranging from 2.95 to 2.99 Å, suggesting that the Zn–Al bond distances found by Voegelin et al. are indicative of Zn sorbed to Al hydroxides, and the Zn–Al bond distances found in this study characteristic of Zn sorbed onto Al edge sites of phyllosilicates. Similar bond distances (3.06–3.09 Å) have been found for the sorption of Zn on the edge sites (magnesium groups) of hectorite [44]. In a study to the sorption mechanisms of Ni onto edge sites of montmorillonite, Dähn et al. [45] showed by using polarized EXAFS spectroscopy that the smaller Ni binds to aluminol edge groups of montmorillonite to 2 Al atoms at 3.00 Å.

The second shell feature in the Zn/goethite sample is best fit with ∼2 Fe atoms at 3.65 Å, suggesting the formation of a bidentate inner sphere sorption complex with hydroxyl groups of the goethite surface. However, the very low surface loading (0.183 μmol/m^2, Table 1) gave rise to a very

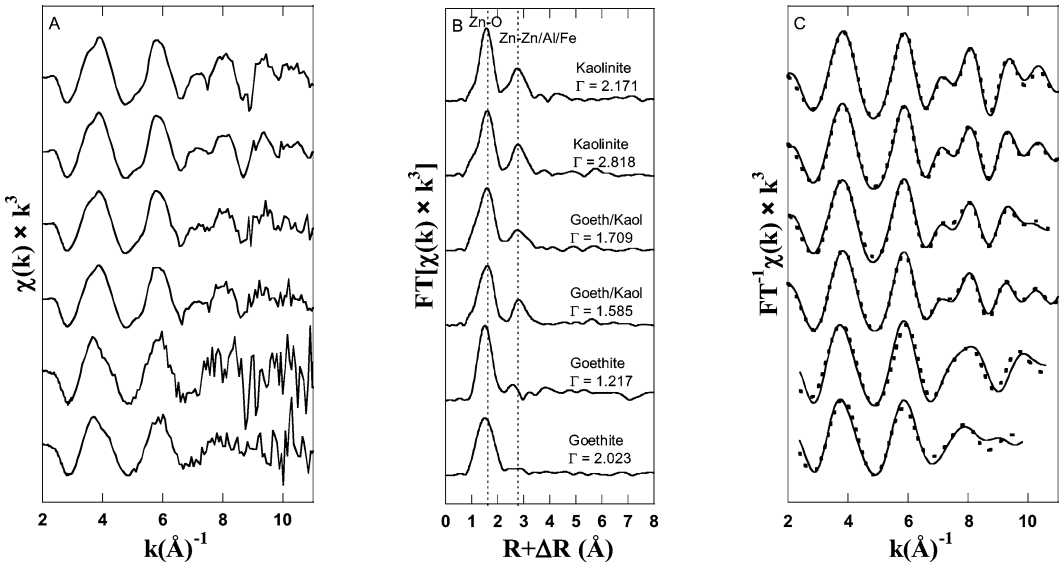

Fig. 4. (A) The k^3-weighted $\chi(k)$ of the high surface loading, pH 7.0 Zn adsorption samples, (B) the corresponding Fourier transforms (not corrected for phase shift), and (C) the fitted inverse Fourier transform of the two first shells of the Fourier transforms, with the solid lines representing the experimental data and the dotted lines the best fits.

noisy spectrum, which leads to a high uncertainty in the fit of the second shell feature. Similarly, Trivedi et al. [24] reported 2–3 Fe atoms at 3.54 Å for Zn sorption to goethite at pH 6.0 and attributed this to the formation of an inner sphere sorption complex. They also reported Zn in tetrahedral coordination with O, while in our system Zn is always in octahedral coordination. These differences in Zn coordination might be caused by differences in crystallinity of the starting material (see discussion for pH 7 sorption samples).

The RSF for the Zn/goethite-coated kaolinite sample displayed a second and a third shell. The second shell is at the same position as the second shell in the Zn/kaolinite spectrum and the third shell is at the same position as in the Zn/goethite spectrum (Fig. 3B), suggesting that Zn sorption in a goethite-coated kaolinite suspension is a combination of Zn sorption on both kaolinite and goethite surfaces. Again, the raw χ spectrum is noisy, due to the low (0.889 µmol/m^2) surface loading. The best fit, but with a high uncertainty, to the backtransformed χ spectrum indicated only two Al atoms at 3.11 Å, suggesting that a bidentate sorption complex is formed with the aluminol edge sites of the kaolinite.

3.3. Zn sorption at pH 7

The raw k^3 weighted χ spectra, their Fourier transforms, and the fitted backtransformed k^3-weigthed spectra of the Zn sorption samples, prepared at pH 7, are shown in Figs. 4 and 5. Zn sorption samples with increasing surface loadings were prepared, representing different regions in the Zn adsorption isotherms (Fig. 2). Different surface loadings were achieved by varying the solid:solution ratio and the reaction time (Table 1). The higher surface loading samples are displayed in Fig. 4. The raw χ spectra of the kaolinite samples and the goethite-coated kaolinite samples look very similar and compare well with the χ spectrum of the synthetic Zn–Al LDH. The similarities in these spectra indicate that Zn containing solid phases, similar in structure to the synthetic Zn–Al LDH, were formed at the kaolinite and the goethite-coated kaolinite surfaces. The raw χ spectra of the Zn/goethite sorption samples are noisy, although reasonable surface loadings were achieved. This may have been caused by Fe fluorescence from the iron oxide degrading the Zn EXAFS signal. The χ spectra of the Zn/goethite sorption samples are distinctly different from the other Zn sorption samples and lack the high frequency patterns found in the

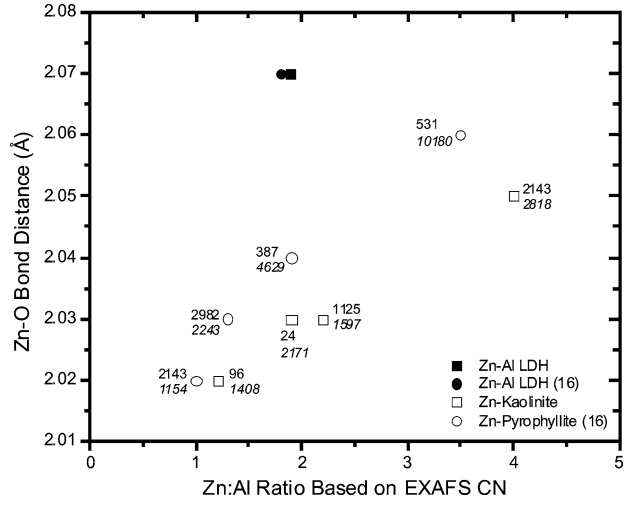

Fig. 5. Comparison of EXAFS-derived Zn–O distance in Zn–Al LDH and sorption samples to Zn–Al ratio calculated by dividing CN_{Zn-Zn} by CN_{Zn-Al}. Reaction time and total Zn solid loading (*italics*, mg/kg) are shown next to the corresponding data points.

other Zn sorption spectra. In fact, the wave frequency is very similar to the ones observed for the pH 5 Zn sorption samples, suggesting that at pH 7, Zn formed an inner sphere sorption complex with hydroxyl groups of goethite, rather than a precipitate phase.

The RSF of the pH 7, high surface loading samples all contain two dominant shells (Fig. 4B). The first shell, at a radial distance of ∼1.8 Å, was fit with ∼6 oxygen atoms at 2.02–2.06 Å, which is indicative of octahedral coordination around the Zn atoms (Table 1). The second shell for the Zn sorbed kaolinite was fit with 3.6 Zn atoms at 3.13 Å, and 0.9 Al atoms at 3.19 Å for the 2.818 µmol/m^2 surface loading sample, and 3.9 Zn at 3.10 Å and 2.6 Al at 3.12 Å for the 2.171 µmol/m^2 sample (Table 1). These bond distances and coordination numbers are in agreement with bond distances found in a study of the Zn sorption mechanisms to pyrophyllite, a 2:1 clay mineral, at pH 7.5 [16]. The only solids that could be formed in our system, sharing the same type of local structure are Zn–Al layered double hydroxide (Zn–Al LDH), Zn phyllosilicate and $Zn_3(OH)_4(NO_3)_2$, of which Zn–Al LDH and Zn phyllosilicate are the most likely phases to form [16]. Unfortunately, neo-formed Zn phyllosilicates and Zn–Al LDH have a very similar structure, and can only be distinguished from each other with polarized EXAFS spectroscopy. In their study, Ford and Sparks [16] observed the formation of a Zn–Al LDH phase at the pyrophyllite surface at every surface loading studied, with an increasing Zn–O bond length with increasing surface loading levels. This increase in Zn–O bond length can also be observed in this study (Fig. 5). This increasing Zn–O bond length was attributed to an increase of the Zn:Al ratio in the octahedral layer with increasing loading levels. The explanation lies in the atomic radii of the atoms. Since the Al atomic radius is smaller than that of Zn, the larger the Zn:Al ratio, the larger the Zn–O and Zn–Zn bond distances have to be to accommodate both Al and Zn in the solid structure. Our results suggest that the number of Al atoms incorporated into the octahedral layer of the Zn–Al LDH surface precipitate is determined by the equilibration time (Fig. 5 and Table 1). The longer the metals are allowed to react with the clay mineral surface, the more Al becomes available by metal promoted dissolution of the clay structure, which can then be incorporated into the neo-formed precipitate. Also, the Zn–O bond lengths corresponding to a certain Zn:Al ratio differed significantly in the synthetic precipitate compared to the solids formed at the clay mineral surfaces (Fig. 5). This can be attributed to the incorporation of other metals (such as structural Fe and Mg from the clay minerals) into the solids formed at the clay mineral surfaces.

Second shell fitting for the Zn/goethite sorbed samples revealed that Zn in the high surface loading sample is bound to 1 Fe atom at 3.18 Å. This result corresponds with the findings of a study by Schlegel et al. [25] to the Zn sorption complexes formed at the goethite surface. At pH 7 they found that Zn, in octahedral coordination, binds to 1 Fe atom at 3.00 Å and 1 Fe atom at 3.20 Å of the goethite surface, corresponding to an edge sharing sorption complex. Contrary to our study and the study by Schlegel et al., Trivedi et al. [24] found that at similar reaction conditions, Zn changed to tetragonal coordination upon binding to 2 Fe atoms at a radial distance of 3.51 Å. The different findings in these three studies may well be related to the crystallinity of the goethite minerals or to the sorption kinetics. In our study we carefully removed any non-crystalline iron oxide with HCl. When goethite is not washed carefully, the surface chemistry of the remaining solid may resemble that of hydrous ferric oxide [31]. In an extensive study on Zn sorption onto ferrihydrite, a hydrous ferric oxide, Waychunas et al. [41] found a change in the Zn coordination environment to tetragonal coordination upon binding two Fe neighbors of the ferrihydrite at a radial distance of 3.44 Å. From a chemical point of view, Zn has a completely filled *d* shell, therefore it does not gain or lose any energy when it changes from octahedral to tetrahedral coordination [40]. Zinc in the sodium nitrate background solution is in octahedral coordination. Therefore it is expected that Zn changes its coordination sphere upon sorption to octahedral goethite only when sorption requires structural rearrangement. Upon changing from an octahedral to a tetrahedral bonding environment, 2 water molecules come off and entropy is gained.

In the lower surface loading sample, Zn was bound to 1.5 Fe or Zn atoms at 3.07 Å. This bond distance is similar to the Zn–Zn distances found in our synthetic Zn–Al LDH and for the precipitate formed at the kaolinite surface. These results suggest that at lower surface loadings, Zn is included in a surface cluster (similar in structure to brucite), while at higher surface loading, Zn forms inner-sphere complexes with goethite. Alternatively, since the low loading sample was aged for 7 days, compared to 1 day for the high loading samples, one could conclude that initially all Zn sorbs to the goethite surface and over time is included into a surface precipitate/cluster, which is thermodynamically favored over an adsorption complex.

As inferred from the raw χ spectra, the Zn sorption complexes formed at the 6 wt% goethite-coated kaolinite surface are very similar to the ones formed at the kaolinite surface. On both the high and the low loading sample, depicted in Fig. 4, a surface precipitate formed: At the lower surface loading, a Zn-hydroxide formed, with 2 Zn atoms in the second shell; at the higher surface loading, a Zn–Al LDH formed with 2.8 Zn and 0.5 Al atoms in the second shell. The total number of atoms in the octahedral layer is lower than the total number of atoms in the octahedral layer of the precipitate phases formed at the kaolinite surface, suggesting that the formation of a surface precipitate is retarded by the presence of a 6 wt% goethite coating. The finding that a Zn–Al LDH phase forms at the kaolinite, and the goethite-coated kaolinite surfaces at pH 7 is significant since this potential metal sequestering mechanism could lead to important contaminant attenuation in certain soil types.

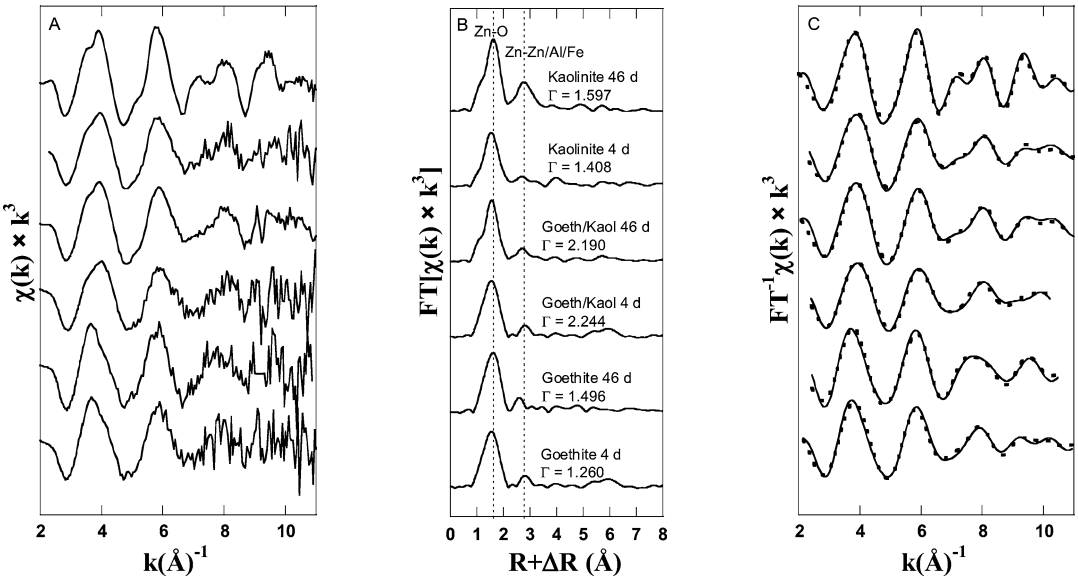

Fig. 6. (A) The k^3-weighted $\chi(k)$ of the time series, pH 7.0 Zn adsorption samples, (B) the corresponding Fourier transforms (not corrected for phase shift), and (C) the fitted inverse Fourier transform of the two first shells of the Fourier transforms, with the solid lines representing the experimental data and the dotted lines the best fits.

3.4. Effect of aging time

Fig. 6 shows the effects of aging time on the Zn sorption complex formed at the different solid surfaces. The initial surface loadings were chosen to be relatively low (Table 1 and Fig. 6). An increase in surface loading at the goethite and kaolinite surface occurs with longer reaction times, and in the case of kaolinite corresponds with an increase in intensity of the second shell in the RSF (Fig. 6B). In the case of goethite, the second shell peak position shifts to lower radial distances with increasing reaction time (Fig. 6B).

Fits to the first shell indicated that Zn sorbed on all three solids was octahedrally coordinated by 5.5–6.6 O atoms at a radial distance of 2.02–2.06 Å. After 4 days, Zn was bound at the kaolinite surface to one Zn atom at 3.10 Å and one Al atom at 3.09 Å. These Zn–Zn/Al distances are again indicative of the presence of a Zn–Al LDH. The low second shell coordination numbers indicate that instead of a fully developed precipitate, a smaller surface cluster may have formed. An increase in the number of atoms in the octahedral layer to 3.9 Zn atoms at 3.11 Å and 1.8 Al at 3.14 Å was recorded for the Zn sorption sample aged for 46 days. This explains the observed increase in intensity of the second shell in the RSF, and is indicative of the growth of a surface precipitate over time.

The shift of the second shell feature in the RSF of the Zn/goethite sorption sample with increasing reaction time to lower radial distances indicates a shift in the major sorption mechanism. The second shell of the 4 day reacted goethite spectrum was fit with one Zn–Fe neighbor at 3.18 Å, which is indicative of a monodentate inner sphere Zn sorption complex (see discussion above). After aging the Zn-reacted goethite suspensions for 46 days, a Zn–Zn/Fe coordination number of 1.2 was found, at a significantly shorter radial distance of 3.07 Å (Table 1). Following the discussion above, only a Zn hydroxide precipitate, similar in structure to brucite, can be formed in our system that shares the same short range order. Our adsorption studies were performed in a nitrogen atmosphere and at concentrations undersaturated with respect to homogeneous precipitation, which excludes the formation of any other solid phase that could potentially share the same short range order. These results confirm the result obtained from the loading samples (Fig. 4), in that Zn binds initially directly to the goethite surface, but over time is incorporated into a Zn hydroxide like surface cluster, suggesting that the incorporation of Zn into a Zn hydroxide phase is thermodynamically more favorable than the formation of adsorption complexes on goethite.

The spectroscopic results of this study provide a plausible explanation for other research [26, and references therein] where an increasing stable metal fraction, with respect to acidification, was observed at the goethite surface after aging the metal reacted goethite. Coughlin and Stone [26] found a rapidly desorbing metal fraction and a slowly desorbing fraction of adsorbed metal upon acidification, with the slowly desorbed fraction increasing in significance with longer aging times for metals such Ni, Co, and Cu, but not for Pb. The labile metal fraction in their study is most likely the adsorbed metal fraction, which decreases over time. Whereas the stable metal fraction represents the metal fraction incorporated into a metal layered double hydroxide (Me–LDH) and increases with reaction time. The ionic radius of Pb is presumably too large to fit into the LDH structure, explaining why it does not show this biphasic desorption behavior. Since Fe^{2+} is not present in our system, this rules out the possible restructuring of the goethite surface into some type of spinel like structure.

Using the same initial solution conditions, much higher Zn surface loadings were achieved at the 10 wt% goethite-coated kaolinite surface compared to the goethite or kaolinite alone. A similar trend was observed in the absorption isotherms (Fig. 2), which suggests that the coated kaolinite complex had a much higher sorption capacity. Some release of Zn was observed after aging the Zn reacted goethite-coated kaolinite for 46 days. This Zn release led to a lower surface loading and suggests a change in the major sorption mechanism. After aging the Zn reacted goethite-coated kaolinite for 4 days, the best fits (Table 1) indicated that the main Zn sorption mechanism is the formation of a monodentate innersphere complex with goethite, with Zn bound to ∼1 Fe atom at 3.19 Å. These results differ from the 6 wt% goethite-coated kaolinite, where the formation of a Zn LDH surface precipitate seemed to be the major sorption mechanism. Thus, the larger amount of goethite at the surface does determine the initial metal sorption behavior of the goethite-coated kaolinite.

Similar to the effect of aging on the Zn sorption complex formed at the goethite surface, after aging the Zn sorption complex formed in the 10.7 wt% goethite-coated kaolinite suspension, a change in the major sorption mechanism takes place. After an incubation time of 46 days, Zn is bound to 1.5 Zn/Fe atoms at 3.11 Å and 0.9 Al atoms at 3.11 Å. This corresponds to the transition from an adsorption complex to the incorporation of Zn into a mixed Zn/Fe–Al LDH surface precipitate.

In conclusion both the extent of the iron oxide coating and the reaction time determine the final Zn sorption complex formed at the goethite-coated kaolinite surface. With a goethite surface coating of 6 wt%, Zn immediately formed a Zn hydroxide precipitate at the kaolinite surface which, with increasing reaction time resembled more a Zn–Al LDH. This suggests that Al became increasingly available over time. In the 10.7 wt% goethite-coated kaolinite suspensions, Zn first formed an inner-sphere sorption complex with the surface hydroxyl groups of goethite. This indicates that goethite had a higher affinity for Zn than the kaolinite clay mineral or the neo-formed precipitate phase. Over time, the inclusion of Zn into a Zn–Al LDH precipitate became the dominant sorption mechanism. This suggests that the formation of a precipitate phase at the kaolinite surface is thermodynamically favored over adsorption on the goethite coating. More studies are needed to determine the effect of reaction kinetics on the sorption complexes formed.

4. Summary

EXAFS spectroscopic studies of the Zn sorption complexes formed at the kaolinite, goethite, and goethite-coated kaolinite surfaces under a range of reaction conditions indicated that at pH 5, Zn formed inner-sphere sorption complexes with all solids studied in this study. A monodentate inner-sphere sorption complex was formed at the kaolinite surface, with Zn binding to Al–OH edge groups at a radial distance of 3.09 Å. Our results suggested that Zn formed a bidentate inner-sphere complex with hydroxyl groups at the goethite surface, with Zn–Fe distances of 3.65 Å. The RSF of the Zn sorption complex formed at the goethite-coated kaolinite surface suggested a combination of the sorption mechanisms of Zn to the individual sorbents, however, only Zn bound to Al–OH edge groups of the kaolinite could be fitted.

The sorption complexes formed at pH 7 changed with surface loading levels and reaction time. At the kaolinite surface, Zn was incorporated into a mixed metal Zn–Al layered double hydroxide already at low loading levels. This neo-formed surface precipitate increased in size with increasing aging time. At the goethite surface, Zn initially formed a monodentate inner-sphere sorption complex, with Zn binding to one Fe atom at 3.18 Å. With increasing reaction time however, the major Zn sorption mechanism changed to the formation of a zinc hydroxide surface precipitate.

Both the extent of the iron oxide coating and the reaction time determined the type of Zn complex formed at the goethite-coated kaolinite surface at pH 7.0. With a surface coating of 6 wt%, Zn was immediately incorporated into a Zn–Al LDH surface precipitate. In the presence of a 10 wt% goethite coating, the initial dominant sorption mechanism was the formation of an inner-sphere sorption complex of Zn with the surface hydroxyl groups of goethite. This indicated that at pH 7.0, goethite has a higher affinity for Zn compared to the kaolinite clay mineral or the surface precipitate. With increasing aging time, the inclusion of Zn into a precipitate phase (similar in structure to brucite) took over as the dominant sorption mechanism. This suggests that the formation of a precipitate phase at the kaolinite surface is thermodynamically favored over adsorption to the goethite coating.

Acknowledgments

This manuscript greatly benefited from the comments and suggestions of two anonymous reviewers. The authors would like to thank Dr. Jeroen Sonke at the High Magnetic Field Lab (Tallahassee, FL) for the ICP-MS analysis, Dr. Matt Eick for the BET surface area measurements, Dr. Kurt Czymmek at the Delaware Biotechnology Institute (Newark, DE) for the SEM analysis and the staff at beamline X11A at the National Synchrotron Light Source, Upton, NY, for their support during the XAFS measurements. Thanks are also extended to M. Gräfe for proofreading the manuscript. This research was funded by the USDA-NRICGP program.

References

[1] G.E. Brown Jr., G.A. Parks, Int. Geol. Rev. 43 (2001) 963.

[2] W. Stumm, J.J. Morgan, Aquatic Chemistry, Wiley, New York, 1996.
[3] M.F. Hochella, in: M.F. Hochella, A.F. White (Eds.), Mineralogical Society of America, Washington, DC, 1990.
[4] D.L. Sparks, Environmental Soil Chemistry, second ed., Academic Press, San Diego, 2003.
[5] J.A. Coston, C.C. Fuller, J.A. Davis, Geochim. Cosmochim. Acta 59 (1995) 3535.
[6] M. Nachtegaal, D.L. Sparks, Environ. Sci. Technol. 37 (2003) 529.
[7] J.M. Zachara, P.L. Gassman, S.C. Smith, D. Taylor, Geochim. Cosmochim. Acta 59 (1995) 4449.
[8] A.S. Templeton, T.P. Trainor, S.J. Traina, A.M. Spormann, G.E. Brown Jr., Natl. Acad. Sci. USA 98 (2001) 11,897.
[9] J.O. Nriagu, J.M. Pacyna, Nature 333 (1988) 134.
[10] A. Manceau, B. Lanson, M.L. Schlegel, J.C. Hargré, M. Musso, L. Eybert-Bérard, J.-L. Hazemann, D. Chateigner, G.M. Lamble, Am. J. Sci. 300 (2000) 289.
[11] D.L. Roberts, A.C. Scheinost, D.L. Sparks, Environ. Sci. Technol. 36 (2002) 1742.
[12] M. Nachtegaal, M.A. Markus, J.E. Sonke, J. Vangronsveld, D. van der Lelie, K. Livi, D.L. Sparks, submitted for publication.
[13] B.J. Alloway (Ed.), Heavy Metals in Soils, Blackie, London, 1990.
[14] J.J.R. Fráusto da Silva, R.J.P. Williams, The Biological Chemistry of the Elements, Oxford Univ. Press, New York, 1991.
[15] R.L. Chaney, in: A.D. Robson (Ed.), Kluwer Academic, The Netherlands, 1993, p. 135.
[16] R.G. Ford, D.L. Sparks, Environ. Sci. Technol. 34 (2000) 2479.
[17] A.M. Scheidegger, G.M. Lamble, D.L. Sparks, J. Colloid Interface Sci. 186 (1997) 118.
[18] H.A. Thompson, G.A. Parks, G.E. Brown Jr., Geochim. Cosmochim. Acta 63 (1999) 1767.
[19] R.G. Ford, A.C. Scheinost, K.G. Scheckel, D.L. Sparks, Environ. Sci. Technol. 33 (1999) 3140.
[20] K.G. Scheckel, A.C. Scheinost, R.G. Ford, D.L. Sparks, Geochim. Cosmochim. Acta 64 (2000) 2727.
[21] U. Schwertmann, P. Cambier, E. Murad, Clays Clay Miner. 33 (1985) 369.
[22] M. Boudeulle, J.P. Muller, Bull. Mineral. 111 (1988) 149.
[23] P. Trivedi, L. Axe, J. Colloid Interface Sci. 244 (2001) 221.
[24] P. Trivedi, L. Axe, J. Colloid Interface Sci. 244 (2001) 230.
[25] M.L. Schlegel, M. Manceau, L. Charlet, J. Phys. IV Fr. 7C-2 (1997) 823.
[26] B.R. Coughlin, A.T. Stone, Environ. Sci. Technol. 29 (1995) 2445.
[27] A. Scheidegger, M. Borkovec, H. Sticher, Geoderma 58 (1993) 43.
[28] T.T. Chao, M.E. Harward, S.C. Fang, Soil Sci. Soc. Proc. 28 (1964) 632.
[29] W.H. Hendershot, L.M. Lavkulich, Soil Sci. Am. J. 47 (1983) 1252.
[30] M.L. Jackson, Soil Chemical Analysis-Advanced Course, University of Wisconsin, Madison, WI, 1956.
[31] D. Peak, R.G. Ford, D.L. Sparks, J. Colloid Interface Sci. 218 (1999) 289.
[32] A. Kandegedara, D.B. Rorabacher, Anal. Chem. 71 (1999) 3140.
[33] R.M. Taylor, Clay Miner. (1984) 591.
[34] T. Ressler, J. Synchrotron Radiat. 5 (1998) 118.
[35] M.J. Eick, S.E. Fendorf, Soil Sci. Soc. Am. J. 62 (1998) 1257.
[36] FEFF Project, 7,02 ed., Department of Physics, University of Washington, Seattle, WA, 1996.
[37] C. Mellini, Am. Mineral. 67 (1982) 587.
[38] A. Munoz-Paez, R.R. Pappalardo, E. Sanchez Marcos, J. Am. Chem. Soc. 117 (1995) 11,710.
[39] M. Hartmann, T. Clark, R. van Eldik, J. Am. Chem. Soc. 119 (1997) 7843.
[40] D.F. Shriver, P.W. Atkins, Inorganic Chemistry, Freeman, New York, NY, 1999.
[41] G.A. Waychunas, C.C. Fuller, J.A. Davis, Geochim. Cosmochim. Acta 66 (2002) 1119.
[42] A. Voegelin, A.C. Scheinost, K. Bühlmann, K. Barmettler, R. Kretzschmar, Environ. Sci. Technol. 36 (2002) 3749.
[43] T.P. Trainor, G.E. Brown Jr., G.A. Parks, J. Colloid Interface Sci. 231 (2000) 359.
[44] M.L. Schlegel, A. Manceau, L. Charlet, J.L. Hazeman, Am. J. Sci. 301 (2001) 798.
[45] R. Dähn, A.M. Scheidegger, M. Manceau, M.L. Schlegel, B. Baeyens, M.H. Bradburry, D. Chateigner, Geochim. Cosmochim. Acta 67 (2003) 1.